

Integrative Taxonomy, Distribution and Ontogenetic Colouration Change in Neotropical Mountain Catfishes of the *Trichomycterus nigroauratus* Group (Siluriformes: Trichomycteridae)

Wilson J. E. M. Costa^{1*}, José Leonardo O. Mattos¹, Sâmela Lopes¹, Pedro F. Amorim¹, and Axel M. Katz¹

¹Laboratory of Systematics and Evolution of Teleost Fishes, Institute of Biology, Federal University of Rio de Janeiro, Caixa Postal 68049, CEP 21941-971, Rio de Janeiro, Brazil. *Correspondence E-mail: wcosta@acd.ufrj.br (Costa). E-mail: jlomattos@gmail.com (Mattos); samelallemos@hotmail.com (Lopes); pedro_f_a@hotmail.com (Amorim); axelmk@gmail.com (Katz)

Received 25 September 2021 / Accepted 28 January 2022 / Published 5 May 2022
Communicated by Felipe Ottoni

Catfishes of the genus *Trichomycterus* comprise the most diverse fish group in mountain river basins crossing the Atlantic Forest of south-eastern Brazil, with a great concentration of species in the Rio Paraíba do Sul basin. The present study is directed to the *T. nigroauratus* group, endemic to the Rio Paraíba do Sul basin, comprising species commonly found associated with bottom leaf litter. Field studies revealed two sympatric, distinct colour morphs, one comprising small specimens with a black longitudinal stripe over a pale brown ground colour on the flank and another comprising a single larger specimen with small dark brown spots scattered over a pale-yellow ground colour. These specimens were found in the upper Rio Paraitinga drainage, an area disjunct from the area inhabited by the other species of the group. We performed coalescent single-locus analyses for species delimitation using a cytochrome *b* fragment (1088 bp) for specimens from eight localities, including sequences taken from specimens exhibiting different colouration morphs and topotypes of all the three nominal species of the *T. nigroauratus* group. The analyses supported the two colouration morphs as belonging to a single species that is herein described. It is distinguished from other congeners by its unique colour pattern, dorsal and anal fins fin more posteriorly placed, and by the morphology of the opercle, metapterygoid and pelvic bone. The Maximum Likelihood analysis indicated the new species as sister to a clade containing all other congeners of the group, which is corroborated by osteological data. The occurrence of different lineages in neighbouring areas of the upper Rio Paraíba do Sul basin is interpreted as a possible vestige of a past complex paleogeographical scenario during the Cenozoic. The present record of striking ontogenetic colouration change, revealed only after checking DNA sequences of individuals exhibiting different colouration phenotypes, again highlights the importance of combining morphological and molecular data in taxonomical studies.

Key words: Atlantic Forest, Mountain biodiversity, Osteology, Rio Paraíba do Sul, Unilocus species delimitation.

BACKGROUND

Tropical mountains shelter a high diversity of endemic species (Hoorn et al. 2013; Antonelli et al. 2018). In south-eastern Brazil, where the landscape is dominated by a series of mountain ranges, the most diverse fish group in mountain rivers is the trichomycterine catfish genus *Trichomycterus* Valenciennes, 1832, with a remarkable concentration of species in the area encompassing the river drainages associated with the upper and middle Rio Paraíba do Sul basin (Costa et al. 2020a b; Vilardo et al. 2020; Costa and Katz 2021). A total of 19 species of the about 60 presently placed in *Trichomycterus* sense Katz et al. (2018), representing four of the five subgenera (Costa 2021), are known to occur in this area, where sometimes five different species are found in sympatry (Costa et al. 2020b).

Evidence from field studies in south-eastern Brazilian mountain rivers has shown that species belonging to different lineages of *Trichomycterus* are specialised in that they inhabit particular riverine environments, such as roots of marginal terrestrial plants, bottom leaf-litter and sandy microhabitats (Costa 1992 2021; Costa et al. 2020a b; Vilardo et al. 2020; Costa and Katz 2021). The *T. nigroauratus* group comprises leaf-litter dwelling species endemic to the Rio Paraíba do Sul basin (Costa et al. 2020b; Costa 2021). The geographical range of the group is situated between the Serra do Mar and Serra da Mantiqueira (Costa et al. 2020b), two parallel mountain ranges with peaks reaching between about 2000 and 2900 m asl, respectively. Among the three species presently included in the group, *Trichomycterus maculosus* Barbosa and Costa, 2010 and *Trichomycterus quintus* Costa, 2020 are relatively rare, occurring in small areas and known from a few specimens deposited in collections (Barbosa and Costa 2010; Costa et al. 2020b). *Trichomycterus maculosus* seems to be endemic to the Rio do Peixe drainage, a left tributary to the upper Rio Paraíba do Sul basin (Barbosa and Costa 2010) and *T. quintus* is only known to occur in the upper Rio Preto drainage, a main tributary of the middle section of the Rio Paraíba do Sul basin (Costa et al. 2020b). The third species of the group, *T. nigroauratus* Barbosa and Costa, 2008, occurs in a broad area comprising tributaries of both margins of the upper Rio Paraíba do Sul basin (Barbosa and Costa 2008). These three species may be readily distinguished by their colour pattern: *T. maculosus* with a series of black spots along flank midline in juveniles, sometimes coalesced to form a black stripe, and a spotted pattern on the flank in adults; *T. quintus* with a uniform black colouration in both juvenile and adults; and *T. nigroauratus* with a black stripe along the flank

midline in juveniles and smaller adults, and a black stripe coalesced to black spots above and below in larger adults (Barbosa and Costa 2008 2010; Costa et al. 2020b). The synapomorphic condition diagnosing the *T. nigroauratus* group is the presence of a folded laminar expansion of the lateral ethmoid border, adjacent to the articular facet for the autopalatine (Costa 2021: fig. 2D).

Between 2001 and 2003, one of us (WJEMC) collected several juveniles and small adults (about 25–50 mm of standard length [SL]) of an undetermined species belonging to the *T. nigroauratus* group, in the upper Rio Paraitinga drainage, the main tributary of the uppermost section of the Rio Paraíba do Sul basin. These specimens had a colour pattern similar to that in juveniles of *T. nigroauratus*. More recently (2020), during a fish collection in the same place, one of us (PFA) found two specimens of this species, one of which had a large size (82.6 mm SL), not observed in previous studies. The colouration of this larger specimen, showing a completely spotted pattern, markedly differed from all other smaller specimens collected in the area, thus not being clear if the larger and smaller specimens were conspecific. The objective of this study was to infer species limits in the *T. nigroauratus* group based on a molecular analysis using a cytochrome *b* fragment (1087 bp) for specimens from eight localities, including sequences taken from the two specimens from the Rio Paraitinga drainage exhibiting different colouration to check if they are conspecific; topotypes of all the three nominal species of the *T. nigroauratus* group; and specimens from other populations of the geographically widespread *T. nigroauratus*, to test their identity.

MATERIALS AND METHODS

Specimens

In addition to old collections cited in previous studies (Barbosa and Costa 2008 2010; Costa et al. 2020b), the present study is based on recent collections from different areas of the upper and middle sections of the Rio Paraíba do Sul basin, which were mainly performed to obtain specimens for DNA extraction. These collections were made with small dip nets (40 × 30 cm) during daylight. Collection permits were provided by ICMBio (Instituto Chico Mendes de Conservação da Biodiversidade; permit number: 38553) and field methods were approved by CEUA-CCS-UFRJ (Ethics Committee for Animal Use of Federal University of Rio de Janeiro; permit number: 065/18). Most specimens were fixed in 10% formalin for a period of 14 days, and then transferred to 70% ethanol. For molecular analyses, whole specimens were fixed

and preserved in 98% ethanol, except specimens of rare species (*i.e.*, the new species herein described), which after euthanasia had a segment of the muscle of the left side of the caudal peduncle dissected, fixed, and preserved in 98% ethanol, while the whole specimen was fixed in 10% formalin as above described. Specimens are deposited in the ichthyological collection of the Institute of Biology of the Federal University of Rio de Janeiro, Rio de Janeiro city, and in the Centre of Agrarian and Environmental Sciences, Federal University of Maranhão, Chapadinha (CICCAA). In lists of specimens, geographical feature names are according to the regional popular use in Portuguese, making it possible to immediately recognize localities in the field and avoiding common errors when translating them to English. Comparative material is listed in Costa (2021). A list of specimens used in the molecular analysis with their respective collecting site coordinates, collection catalogue numbers, and GenBank accession numbers appears in table 1.

Morphological data

Data on colouration are based on photographs of live individuals taken a few hours after collection and melanophore patterns analysed in preserved specimens. Morphometric data were taken following Costa (1992), with modifications proposed by Costa et al. (2020a). Meristic data followed Bockmann and Sazima (2004), using the following formula in the descriptions: lower case roman numerals indicating unsegmented unbranched rays; upper case numerals indicating segmented unbranched rays; and Arabic numerals indicating segmented branched rays. Vertebra counts include all free vertebrae, with the compound caudal centrum counted as a single element, and

exclude those contained in the Weberian apparatus. Cephalic laterosensory system terminology followed Bockmann and Sazima (2004). Specimens were cleared and stained for bone and cartilage (C&S in lists of specimens) following Taylor and Van Dyke (1985). Osteological characters included in descriptions refer to structures with informative variability in closely related species of *Trichomycterus* (Costa et al. 2020a b; Vilardo et al. 2020), including the mesethmoidal region, suspensorium, opercular apparatus, and gill arches, besides the pelvic girdle morphology that is useful to distinguish the new species. Osteological nomenclature is according to Costa (2021). Osteological illustrations were made using a stereomicroscope Zeiss Stemi SV 6 with camera lucida. Bone measurements are according to Costa and Katz (2021).

DNA extraction, amplification and sequencing

Total genomic DNA was extracted from muscle tissues of the right side of the caudal peduncle and dorsum using the DNeasy Blood & Tissue Kit (Qiagen), following the manufacturer's protocol. The analyses included a fragment of the mitochondrial encoded gene cytochrome *b* (CYTB); amplification was made through the polymerase chain reaction (PCR) method, using the primers Cytb Siluri F (5'-CCA CCG TTG TAA TTC AAC TA-3') and Cytb Siluri R (5'-GAT TAC AAG ACC GGC GCT TT-3') (Villa-Verde et al. 2012). Double-stranded PCR amplifications were performed in 60 µl reactions with reagents at the following concentrations: 5× GreenGoTaq Reaction Buffer (Promega), 1.5 mM MgCl₂, 1 mM of each primer, 75 ng of total genomic DNA, 0.2 mM of each dNTP and 1 U of Promega GoTaq DNA polymerase. The thermocycling profile was as follows: initial denaturation for 4 min at 95°C;

Table 1. Terminal taxa used in the phylogenetic analysis and their respective GenBank accession numbers

Species	Access number	Voucher	Locality	Coordinates
<i>Trichomycterus septemradiatus</i>	MW196781	UFRJ9888	Conceição da Aparecida, MG	24°04'24"S, 46°12'04"W
<i>Trichomycterus mirissumba</i>	MW196761	UFRJ11978	Bocaina de Minas, MG	22°14'48"S, 44°31'19"W
<i>Trichomycterus immaculatus</i>	MK144348	UFRJ10001	Lima Duarte, MG	21°48'30"S, 43°49'17"W
<i>Trichomycterus maculosus</i>	MN813002	UFRJ12340	São José dos Campos, SP	22°55'30"S, 45°58'50"W
<i>Trichomycterus nigrauratus</i>	OK247569	UFRJ10305.1	São José do Barreiro, SP	22°40'24"S, 44°34'50"W
	OK247570	UFRJ10305.2	São José do Barreiro, SP	22°40'24"S, 44°34'50"W
	OK247571	UFRJ10308.1	Piquete, SP	22°35'14"S, 45°12'38"W
	OK247572	UFRJ10315.1	Resende, RJ	22°23'58"S, 44°31'20"W
	OK247573	UFRJ12357.1	Resende, RJ	22°25'30"S, 44°44'3"W
	OK247574	UFRJ12022.1	Bocaina de Minas, MG	22°19'26"S, 44°34'57"W
<i>Trichomycterus quintus</i>	OK247575	UFRJ12037.1	Itatiaia, RJ	22°19'43"S, 44°34'05"W
	OK247576	UFRJ12641	Cunha, SP	23°09'26"S, 44°51'21"W
<i>Trichomycterus mutabilicolor</i>	OK247577	UFRJ12642	Cunha, SP	23°09'26"S, 44°51'21"W

35 cycles of denaturation for 40 sec at 94°C, annealing for 30 s at 60°C and extension for 1.5 min at 72°C; and terminal extension for 4 min at 72°C. Negative controls were used to check DNA contaminations. The PCR products were purified using the Wizard SV Gel and PCR Clean-Up System (Promega). Sanger Sequencing reactions were made by Instituto SENAI de Inovação em Biossintéticos. Sequencing chromatograms and sequences were assessed using MEGA 7 (Kumar et al. 2018). The generated DNA sequences were translated into amino acids residues to verify the absence of premature stop codons or indels using the program MEGA 7.

Phylogenetic analyses and species delimitation

The analyses were performed using a CYTB fragment 1088 bp for ten specimens belonging to the *T. nigroauratus* species group collected in eight sites, including topotypes of all the three nominal species, and three outgroup species, including *T. immaculatus* (Eigenmann and Eigenmann, 1889), a species of the *T. nigricans* group, which is sister to the *T. nigroauratus* species group (Costa et al. 2020b; Costa 2021), *T. mirissumba* Costa, 1992, a member of a clade that is sister to the clade containing the *T. nigroauratus* and *T. nigricans* groups (Costa et al. 2020b; Costa 2021), and *T. septemradiatus* Katz, Barbosa and Costa, 2013, a species of a basal clade of *Trichomycterus* sense Katz et al. (2018), the *T. reinhardti* group (Costa 2021; Costa and Katz 2021). A list of specimens with their respective collecting coordinates and GenBank accession numbers is provided in table 1.

The best partition scheme and best-fit models of substitution for the data set were inferred using PartitionFinder 2.1.1 (Lanfear et al. 2016) according to the Bayesian information criterion (BIC; Schwarz 1978), which indicated partitioning by codon position, and the following substitution models: K80+I, HKY and TRN+G, respectively, for each gene codon position. The following topology reconstruction methods were implemented: the Bayesian inference was performed with BEAST v.1.10.4 (Suchard et al. 2018), using an uncorrelated relaxed lognormal model, a skyline coalescent tree prior, following Ritchie et al. (2017), and other parameters set as default; the MCMC length was 50,000,000 runs with sampling every 1000 runs. The quality of the MCMC chains was evaluated in Tracer 1.7.1 (Rambaut et al. 2018); a 25% burn-in was removed and the final tree was obtained using TreeAnnotator v.1.10.4 from BEAST v.1.10.4 package; support values of the Bayesian inference (BI) analysis were calculated by posterior probability. The Maximum

Likelihood was performed with IQ-TREE 2.0 software (Nguyen et al. 2015; Chernomor et al. 2016), support of the nodes was evaluated by the calculation of 1000 ultrafast bootstrap (Hoang et al. 2018), and 1000 bootstrap (Felsenstein 1985) replicates.

Coalescent single-locus models for species delimitation were: the Bayesian implementation of Poisson Tree Process (bPTP) (Zhang et al. 2013), with 500,000 Markov chain Monte Carlo (MCMC) generations, thinning set to 100 and a burn-in of 25% initial samples, checking both Maximum likelihood and Bayesian solutions; and the Generalized Mixed Yule-Coalescent (GMYC) (Fujisawa and Barraclough 2013), independently applying both single and multiple-threshold. All analyses just included different haplotypes and were carried on the Exelixis Lab's web server (GMYC at <http://species.h-its.org/gmyc/>; bPTP at <http://species.h-its.org/ptp/>).

RESULTS

Comparative morphology, phylogenetic relationships and species delimitation

Examination of external morphological characters (i.e. fin and latero-sensory system morphology) did not provide any informative character distinguishing specimens of the two colour morphs from the Rio Paraitinga. On the other hand, molecular data indicated that these specimens are conspecific. All the four analyses supported delimitation of four species (Fig. 1): the three species previously described, including the geographically widespread *T. nigroauratus*, and a new species that is formally described below, comprising the population from the upper Rio Paraitinga drainage. The new species is morphologically diagnosable by osteological data (see diagnosis below).

A clade including only *T. maculosus* and *T. nigroauratus* was supported by high values in both analyses, but relationships between *T. quintus* and the new species were weakly supported, showing incongruent results in each analysis. In the BI analysis, *T. quintus* appeared as sister to the other congeners of the group, whereas in the ML analysis, *T. quintus* is supported as sister to a clade comprising *T. maculosus* and *T. nigroauratus* (Fig. 1).

TAXONOMY

Family Trichomycteridae Bleeker, 1858
Genus *Trichomycterus* Valenciennes, 1832

***Trichomycterus mutabilicolor* Costa, sp. nov.**

(Figs. 2, 3C, D, 4; Table 2)

urn:lsid:zoobank.org:act:A02C0F12-B107-4662-AF6B-1AB26976BEE9

Holotype: UFRJ 12650, 82.6 mm SL; Brazil: São Paulo state: Cunha municipality: Cachoeira Mato Limpo, Riacho Pedacinho do Céu, a tributary of the Rio Taboão, which is a tributary of the Rio Manso, itself a tributary of the Rio Monjolo, upper Rio Paraitinga drainage, Rio Paraíba do Sul basin, 23°09'25"S 44°51'21"W, altitude about 1335 m asl; B. Mesquita and P.F. Amorim, 25 January 2020.

Paratypes: All from Brazil: São Paulo state: Cunha municipality: upper Rio Paraitinga drainage, Rio Paraíba do Sul basin. – UFRJ 12649, 37.3 mm SL; collected with holotype. – UFRJ 5697, 1, 47.9 mm SL; same locality as holotype; W. J. E. M. Costa, B. B. Costa and C. P. Bove, 8 March 2003. UFRJ 5652, 2, 36.0–40.7 mm SL; UFRJ 5696, 1, 38.1 mm SL (C&S); same locality as holotype; W. J. E. M. Costa, B. B. Costa and C. P. Bove, 14 April 2001. – UFRJ 5698, 7, 26.8–43.8 mm SL; CICC AA 02712, 4, 27.8–35.2 mm SL; UFRJ 5699, 3 (C&S), 37.2–47.4 mm SL; Toca das Andorinhas, Rio Monjolo, Rio Paraitinga drainage, Rio Paraíba do Sul basin, 23°06'08"S 44°51'56"W, altitude about 1200 m asl; W. J. E. M. Costa, B. B. Costa and C. P. Bove, 6 March 2003. – UFRJ 5700, 8, 33.2–45.7 mm

SL; UFRJ 5625, 4, 34.1–56.6 mm SL (C&S); same locality and collectors as UFRJ 5698, 17 April 2001.

Diagnosis: *Trichomycterus mutabilicolor* is a member of the *T. nigroauratus* group, which is easily diagnosed by the presence of a folded laminar expansion of the lateral ethmoid border, just above the articular facet for the autopalatine (Fig. 4A; vs. absence). *Trichomycterus mutabilicolor* differs from all other species of the *T. nigroauratus* group by its flank colouration (brownish grey with a black stripe between snout and caudal fin base in specimens between about 26.8 and 56.6 SL length (Fig. 3C), and body yellowish grey with small dark brown spots in a specimen 82.6 mm SL mm SL (holotype, Fig. 3D); vs. juveniles with a series of black elongate spots along body midline, sometimes coalesced to form a stripe, and adults with grey spots over pale brownish grey spots on flank in *T. maculosus*, always homogeneously black in *T. quintus*, and a persistent black stripe in large specimens of *T. nigroauratus*), dorsal and anal fins fin more posteriorly placed relative to vertebrae counts (dorsal-fin origin at a vertical through the centrum of the 20th or 21nd vertebra, and the anal-fin origin at a vertical through the centrum of the 24th or 25th vertebra; vs. dorsal-fin origin at a vertical between the centrum of the 17th and the 19th vertebra, and the anal-fin origin at a vertical through the centrum of 22nd or 23rd vertebra), metapterygoid deeper than long (Fig. 4B; vs. longer

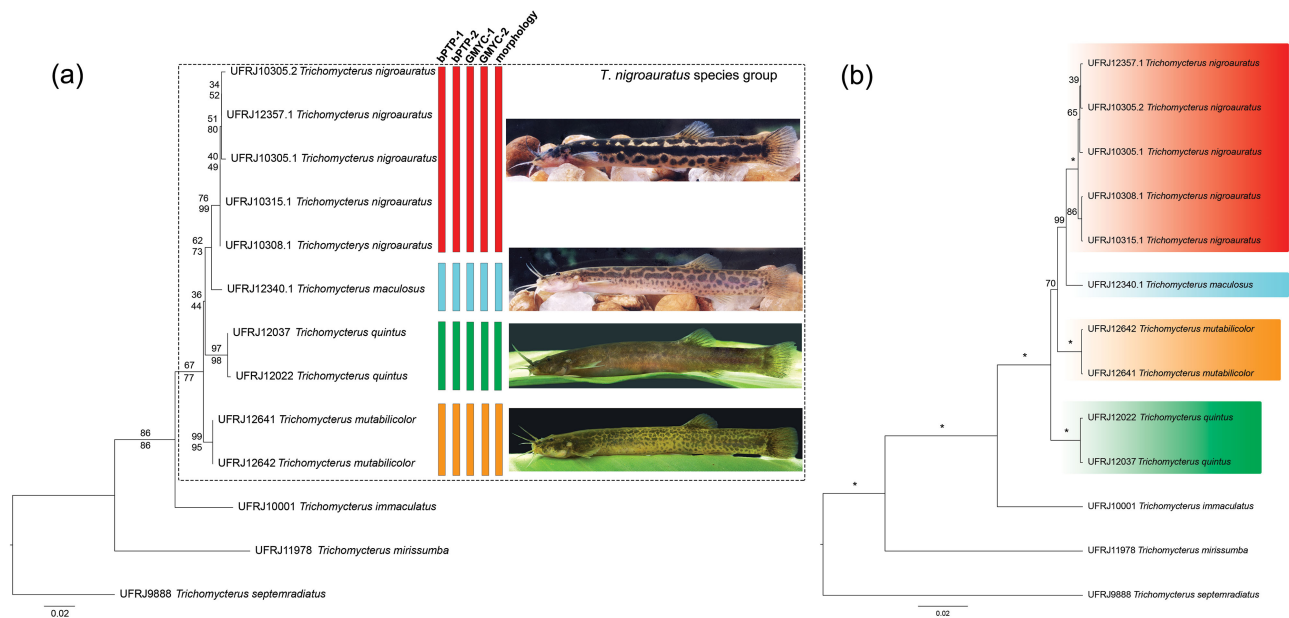


Fig. 1. Phylogenetic trees used to delimit species, using sequences of the mitochondrial gene cytochrome *b*, 1088 bp, for 10 sequenced individuals belonging to eight populations of the *Trichomycterus nigroauratus* group and three outgroups. (a) tree generated by Maximum Likelihood (numbers above and below branches are bootstrap and fast bootstrap values, respectively; bars are species delimitation results relative to: bPTP, Bayesian implementation of Poisson Tree Process, using: 1, Maximum likelihood, and 2, Bayesian solutions; GMYC, Generalized Mixed Yule-Coalescent, using: 1, single, and 2, multiple threshold options); (b) tree generated by Bayesian inference (numbers above nodes are posterior probability values above 0.70; asterisks represent maximum values). Taxon names are preceded by UFRJ catalogue numbers.

than deep, Costa 2021: fig. 3D), a thicker opercle, with a short ventral process (Fig. 4B; vs. thinner, with relatively long ventral process, Costa 2021: fig. 3D); and a broad pelvic bone, its length excluding processes slightly longer than its width (Fig. 4D; vs. narrow, its length about three or four times its width, Costa 2021: fig. 6D).

Description: Morphometric data appear in table 1. Largest specimen examined 82.6 mm SL. Body moderately slender, subcylindrical and slightly depressed anteriorly, compressed posteriorly. Greatest body depth at vertical midway between pectoral and pelvic fin base. Dorsal profile of head and trunk slightly convex, approximately straight on caudal peduncle; ventral profile straight to slightly convex between lower jaw and anal-fin base end, straight on caudal peduncle. Anus and urogenital papilla at vertical through anterior third of dorsal-fin base. Head trapezoidal in dorsal view. Head surface with minute skin papillae. Anterior profile of snout slightly convex in dorsal view. Eye small, dorsally positioned in head. Posterior nostril located nearer anterior nostril than orbital rim. Tip of maxillary barbel reaching between anterior and middle portion of opercular patch of odontodes; tip of rictal barbel reaching anterior portion of interopercular patch of odontodes; tip of nasal barbel reaching between posterior margin of orbit and point midway between orbit and opercular patch of odontodes. Mouth subterminal. Jaw teeth pointed in specimens 50 mm SL

or smaller, incisiform in holotype; teeth arranged in 3 or 4 irregular rows. Branchial membrane attached to isthmus only at its anterior point. Branchiostegal rays 7 or 8.

Dorsal and anal fins subtriangular; total dorsal-fin rays 11 or 12 (iii + II + 6–7), total anal-fin rays 10 (iii + II + 5). Anal-fin origin at vertical through posterior extremity of dorsal-fin base. Dorsal-fin origin at vertical through centrum of 20th or 21st vertebra, anal-fin origin at vertical between centrum of 24th or 25th vertebra. Pectoral fin subtriangular in dorsal view, posterior margin slightly convex, first pectoral-fin ray terminating in filament reaching about 30% of pectoral-fin length without filament; total pectoral-fin rays 8 (I + 7). Pelvic fin truncate, its posterior extremity reaching urogenital papilla; pelvic-fin bases medially separated by small interspace; total pelvic-fin rays 5 (I + 4). Caudal fin truncate, posterior margin nearly straight, upper and lower corners rounded; total principal caudal-fin rays 13 (I + 11 + I), total dorsal procurrent rays 16–19 (xv–xviii + I), total ventral procurrent rays 13–16 (xii–xv + I). Vertebrae 37–39. Ribs 13 or 14. Two dorsal hypural plates, corresponding to hypurals 4 + 5 and 3, respectively; single ventral hypural plate corresponding to hypurals 1 and 2 and parhypural.

Laterosensory system: Supraorbital sensory canal continuous, connected to posterior section of infraorbital canal posteriorly. Supraorbital sensory canal with 3 pores: s1, adjacent to medial margin of

Table 2. Morphometric data of *Trichomycterus mutabilicolor* Costa sp. nov.

	holotype	paratypes (<i>n</i> = 6)
Standard length (mm)	82.6	36.0–45.7
Percent of standard length		
Body depth	11.0	11.0–16.0
Caudal peduncle depth	11.7	9.7–12.7
Body width	10.7	8.4–11.4
Caudal peduncle width	2.7	1.9–2.9
Pre-dorsal length	63.8	61.6–64.4
Pre-pelvic length	57.8	58.5–61.1
Dorsal-fin base length	11.2	10.5–13.7
Anal-fin base length	6.9	7.9–12.0
Caudal-fin length	15.0	15.0–20.2
Pectoral-fin length	13.0	13.3–17.0
Pelvic-fin length	9.8	9.1–11.5
Head length	21.0	21.6–23.2
Percent of head length		
Head depth	41.7	42.1–46.7
Head width	87.8	79.5–91.9
Snout length	47.2	41.0–46.6
Interorbital length	25.9	25.7–31.5
Preorbital length	15.7	11.8–15.2
Eye diameter	10.9	14.0–16.3

anterior nostril; s3, adjacent and just posterior to medial margin of posterior nostril; and s6, at transverse line through posterior half of orbit; s6 nearer to its lateral homologous pore than to orbit. Infraorbital sensory canal arranged in 2 segments, each with two pores; anterior segment with pore i1, at transverse line through anterior nostril, and pore i3, at transverse line just anterior to posterior nostril; posterior segment with pore i10, adjacent to ventral margin of orbit, and pore i11, posterior to orbit. Postorbital canal with 2 pores: po1, at vertical line above posterior portion of interopercular patch of odontodes, and po2, at vertical line above posterior portion of opercular patch of odontodes. Lateral line of body short, with 2 pores, posterior-most pore at vertical just posterior to pectoral-fin base.

Mesethmoidal region and adjacent structures (Fig. 4A): Anterior margin of mesethmoid gently concave, mesethmoid subcylindrical. Antorbital thin, approximately elliptical in dorsal view. Sesamoid supraorbital elongate, rod-like, without lateral

processes, its length about two times and half antorbital length. Premaxilla long, subrectangular, narrowing laterally. Maxilla boomerang-shaped, slender, about equal to premaxilla in length or slightly longer, almost straight, posterior process rudimentary. Autopalatine subrectangular in dorsal view when excluding posterolateral process, broad, its shortest width about half autopalatine length, lateral margin nearly straight, medial margin slightly concave; latero-posterior process of autopalatine triangular, short, its length about two thirds autopalatine length. Dorsal surface of autopalatine about plain, without distinctive ridges. Autopalatine articular facet for lateral ethmoid shell-shaped dorsally, without processes, articular facet for vomer minute. Distinctive flap close mesethmoid articular facet for autopalatine. Anterodorsal extremity of lateral ethmoid with slight lateral expansion. Lateral margin of lateral ethmoid continuous, without processes.

Suspensorium and opercular apparatus (Fig. 4B): Metapterygoid subtriangular, deeper than long,



Fig. 2. *Trichomycterus mutabilicolor* Costa sp. nov., UFRJ 12650, holotype, 82.6 mm SL. (a), left lateral view; (b), dorsal view; (c), ventral view.

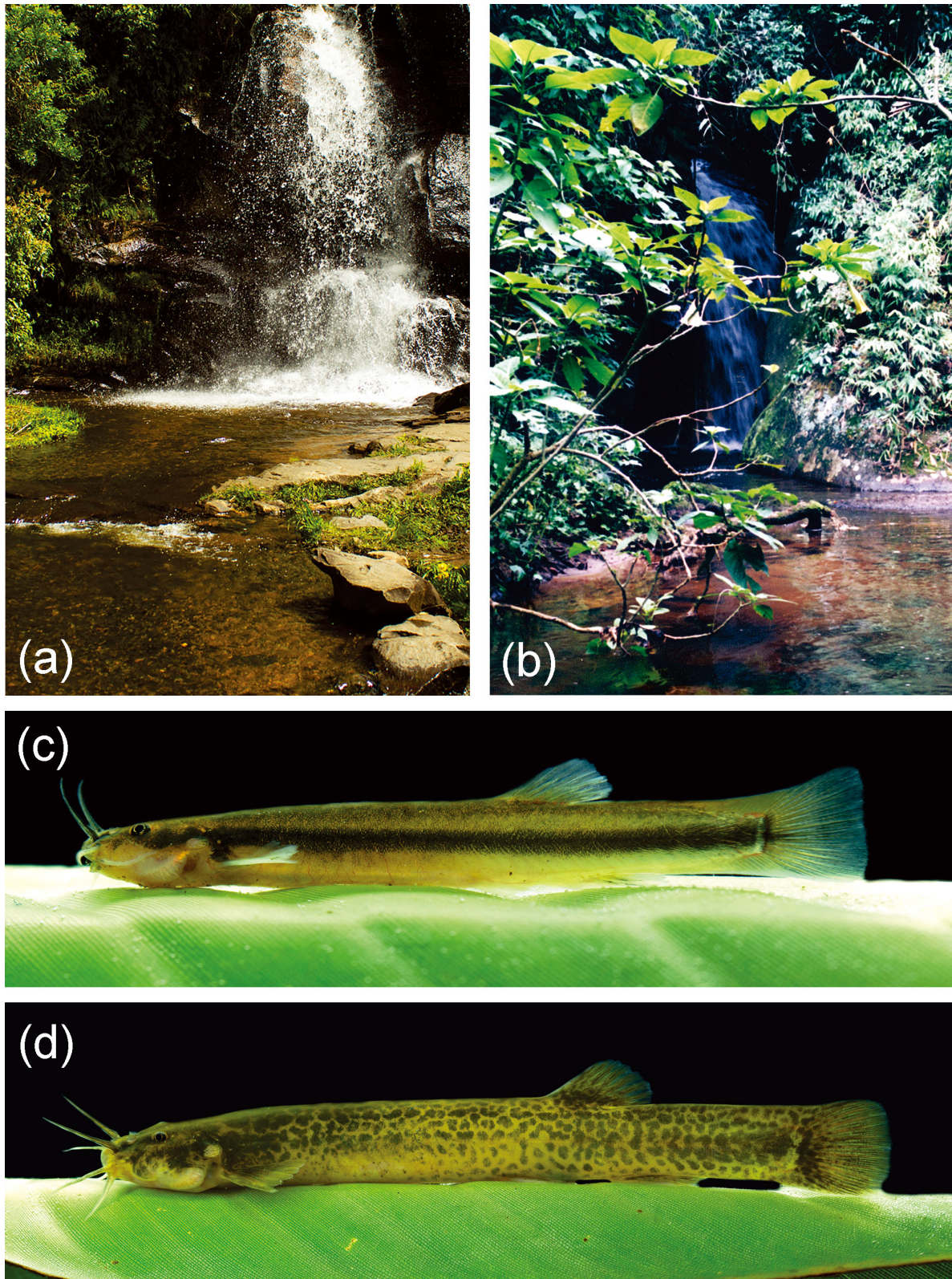


Fig. 3. Habitat and live colouration of *Trichomycterus mutabilicolor* Costa sp. nov. (a), Cachoeira Mato Limpo, Riacho Pedacinho do Céu, upper Rio Paraitinga drainage, the type locality (23°09'25"S 44°51'21"W); (b) Toca das Andorinhas, Rio Monjolo, upper Rio Paraitinga drainage (23°06'08"S 44°51'56"W); (c) UFRJ 12649, 37.3 mm SL, paratype, DNA sequence used in the molecular analysis; (d) UFRJ 12650, 82.6 mm SL, holotype, DNA sequence used in the molecular analysis.

anterior margin curved, posterior portion terminating in slender extension. Quadrate robust, dorsoposterior outgrowth in close proximity to hyomandibula anterior outgrowth. Hyomandibula long, with well-developed anterior outgrowth; middle portion of dorsal margin of hyomandibula outgrowth. Opercle moderately robust, depth of opercular patch of odontodes about three quarters of length of dorsal articular cartilage of hyomandibula; dorsal process of opercle short and blunt, about half opercle length; ventral process supporting ligamentous connections to interopercle short; well-developed flaps adjacent to articular facets for hyomandibula and preopercle. Opercular odontodes 16–20; odontodes pointed, straight to slightly curved, arranged in irregular transverse rows. Interopercle long, about four fifths of hyomandibula length; dorsal interopercular process constricted at its base, anteriorly expanded on its dorsal tip. Interopercular odontodes 35–44; odontodes pointed, about straight, arranged in irregular longitudinal rows. Preopercle compact, with short ventral projection.

Branchial arches (Fig. 4C): Basibranchials 2 and 3 subcylindrical, basibranchial 2 slightly shorter and wider than basibranchial 3; basibranchial 4 cartilage sub-triangular, wider than long. Hypobranchial 1 subcylindrical, abruptly widening at its lateral tip; hypobranchial 2 subtriangular, osseous portion longer than cartilaginous portion; hypobranchial 3 subtrapezoidal, osseous portion small and narrow, cartilaginous portion broad. Ceratobranchial 1 broad in its proximal tip, gradually narrowing to its distal tip; ceratobranchials 2 and 3 widened in their middle portion, with shallow concavity on posterior margin of basal portion; ceratobranchial 4 sub-rectangular; ceratobranchial 4 accessory cartilage minute;

ceratobranchial 5 boomerang-shaped, its largest width nearly equal to width of ceratobranchial 4; 23–25 small, slightly curved teeth on ceratobranchial 5 tooth patch. Epibranchial 1 slender, with well-developed sharp anterior uncinat process; epibranchial 2 slender, with rudimentary anterior uncinat process; epibranchial 3 slender, with well developed, curved posterior uncinat process; epibranchial 4 broad, sub-rectangular, proximal portion broader than distal portion. Pharyngobranchial 3 short, subcylindrical; pharyngobranchial 4 longer, slightly curved; 20–22 small, curved teeth on pharyngobranchial 4 dentigerous plate.

Pelvic girdle (Fig. 4D): Pelvic bone broad, its length excluding processes slightly longer than its width; external and internal anterior processes similar in length, longer than pelvic bone excluding processes; antero-medial process well-developed, about one quarter to one third internal anterior process length; posterior process well-developed, about straight, posteriorly directed.

Colouration in life (Fig. 3C–D): In juvenile specimens, between about 25 and 40 mm SL (Fig. 3C), trunk and head light brownish grey, with mid-lateral black stripe between post-orbital area and caudal peduncle end; ventral surface of trunk and head light grey. Opercular and interopercular patches of odontodes light grey. Nasal barbel brown, maxillary and rictal barbels grey. Iris dark brown, with narrow pale-yellow line around pupil. Fins hyaline, with melanophores concentrated on mid-basal portion of caudal fin. Specimens between about 45 and 55 mm SL, similar to juvenile specimens, but stripe lighter, and with faint brown spots above flank stripe and minute brown dots below. In large specimen, 82.6 mm SL (holotype, Fig. 3D), trunk and head pale brownish yellow, with

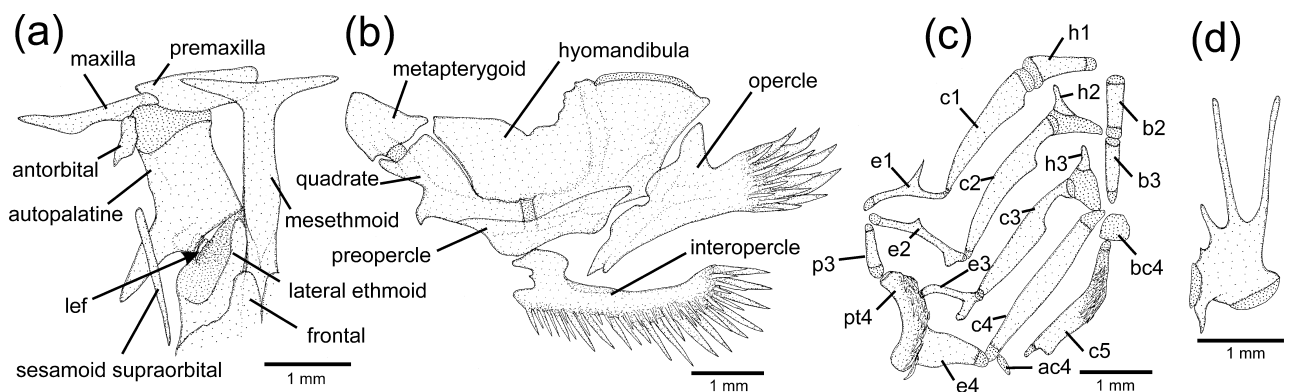


Fig. 4. Osteological structures of *Trichomycterus mutabilicolor* Costa sp. nov. (a), mesethmoidal region and adjacent structures, middle and left portion, dorsal view; (b), left jaw suspensorium and opercular apparatus, lateral view; (c), middle and left portion of branchial arches, ventral view of dorsal elements on left, dorsal view of ventral elements on right; (d), left pelvic bone, ventral view. Abbreviations: ac4, accessory cartilage basibranchial 4; b2–3, basibranchials 2–3; bc4, cartilaginous basibranchial 4; c1–5, ceratobranchials 1–5; e1–4, epibranchials 1–4; h1–3, hypobranchials 1–3; p3, pharyngobranchial 3; lef, lateral ethmoid flap; pt4, pharyngobranchial 4 tooth-plate. Larger stippling represents cartilages.

small dark brown spots, more concentrated on head, anterior portion of flank and mid-posterior portion of caudal peduncle; ventral surface of trunk and head light yellowish grey. Opercular and interopercular patches of odontodes light grey. Nasal barbel brown, maxillary and rictal barbels yellowish grey. Iris dark brown, with narrow pale-yellow line around pupil. Fins yellowish hyaline, with great concentration of dark brown spots on basal portion.

Colouration in alcohol: Similar to life colouration, but with pale colours.

Etymology: From the Latin *mutabilicolor* (changing colour), referring to the striking ontogenetic colouration change.

Distribution and habitat notes: *Trichomycterus mutabilicolor* is known from two sites in the upper section of the Rio Paraitinga drainage, Rio Paraíba do Sul basin, in altitudes between 1200 and 1335 m asl (Fig. 5). The water was clear and river bottom comprised rocks, gravel and sand (Fig. 3A–B). Specimens of the type series were collected within leaf litter just below waterfalls, about 40–80 cm depth.

DISCUSSION

Phylogenetic relationships

Both phylogenetic analyses supported *T. maculosus* and *T. nigroauratus* as sister taxa, but the phylogenetic position of *T. mutabilicolor* and *T. quintus* were different and weakly supported, with *T. mutabilicolor* in ML and *T. quintus* in BI as sister to all other congeners of the *T. nigroauratus* group. However, osteological data corroborates *T. mutabilicolor* as sister to all other species of the group, since *T. maculosus*, *T. nigroauratus*, and *T. quintus* share three derived character states that are not present in *T. mutabilicolor*. In these three species, the opercle is thin and bears a relatively long and slender ventral process, longer than the opercular dorsal process (Costa 2021: fig. 3D), the metapterygoid has a posterior expansion (Costa 2021: fig. 3D), and the pelvic bone is slender, with its width at the middle portion about one third to one quarter its length (Costa 2021: fig. 6D). In *T. mutabilicolor*, the opercle and the pelvic bone are considerably more

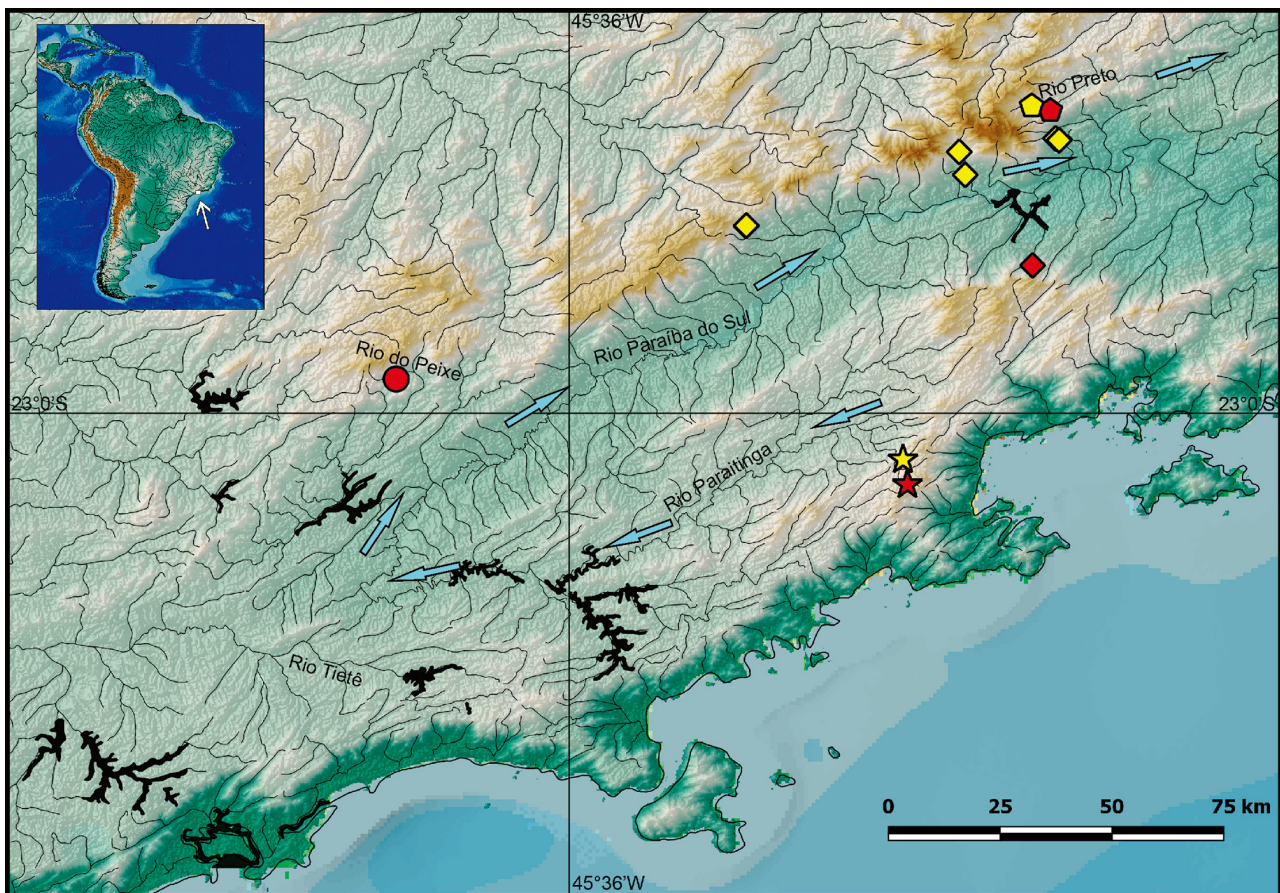


Fig. 5. Geographical distribution of the *Trichomycterus nigroauratus* group. Dot, *T. maculosus*; lozenges, *T. nigroauratus*; pentagons, *T. quintus*; stars, *T. mutabilicolor* Costa sp. nov. Red symbols indicate type localities. Arrows indicate the direction of the main river flow.

compact, with the opercular ventral process shorter than the dorsal process ventral and the pelvic bone width at its middle portion larger than the length (Fig. 4B, D), as similarly occurring in members of other generic lineages (see Costa 2021: figs. 3 and 6 for opercle and pelvic bone morphology, respectively, among lineages of *Trichomycterus*), thus parsimoniously interpreted as plesiomorphic conditions. The metapterygoid of *T. mutabilicolor* is deeper than long, not forming a distinctive posterior process, which seems to be the plesiomorphic condition for *Trichomycterus* (Costa 2021), thus differing from other species of the *T. nigroauratus* group, as well as species of the *T. nigricans* group that have a metapterygoid that is longer than deep (Costa 2021: fig. 3D).

Distribution patterns

Although all species of the *T. nigroauratus* group are endemic to the Rio Paraíba do Sul basin, the distribution area of *T. mutabilicolor* in the upper Rio Paraitinga drainage may be considered disjunct from the broad area occupied by the other congeners, since the main course of the Rio Paraitinga runs to southwest, whereas other congeners inhabit areas of the Paraíba do Sul basin where the main courses run to northeast (Fig. 5). This distribution pattern is probably a result of a past complex paleogeographical scenario. According to available models, the area presently comprising the upper Rio Paraíba do Sul and the adjacent upper Rio Paraná basin (*i.e.*, Rio Tietê drainage) drastically changed during the Cenozoic (Ribeiro 2006), when some drainages were successively captured by other neighbouring drainages to form a long taphrogenic basin system (*i.e.*, the Taubatê basin) before reaching the present basin configuration. Therefore, the occurrence of different lineages occurring in the upper Rio Paraíba do Sul basin may be a vestige of past biogeographical events prior to the formation of the present Rio Paraíba do Sul basin, but further time-calibrated phylogenetic analyses are necessary to test this hypothesis.

Colouration

Ontogenetic colouration change has been reported to occur in eastern South American trichomycterines (Miranda Ribeiro 1905; Bockmann and Sazima 2004; Ferrer and Malabarba 2013; Vilardo et al. 2020). In these taxa, colouration change is gradual and slight, never so intense as in *T. mutabilicolor*. On the other hand, striking ontogenetic colouration change has also been reported for some trichomycterines from northern South America and southern Central America (*e.g.*, Ardila Rodríguez 2011; Angulo et al. 2018). Although

colouration change may be associated with habitat change during ontogeny, with juveniles and larger adults occurring in different habits as suggested in some field studies on other trichomycterids (Sazima 2004; Zanata and Primitivo 2013), little is known about similar habitat changes in trichomycterines. Considering that numerous specimens of *T. mutabilicolor* about 25–50 mm SL were easily found in different collecting trips, whereas only one large specimen 82.6 mm SL exhibiting that unique colouration was collected, it would be plausible that larger specimens were not easily accessible to fish collectors in the sampled habitats, probably preferentially inhabiting sites not still sampled. However, further field studies are needed to check if larger specimens of *T. mutabilicolor* in fact occur in different habitats.

CONCLUSIONS

The integrative use of morphological and molecular data in studies on the species rich Trichomycterinae clade has provided robust and quick advances in its classification (*e.g.*, Costa and Katz 2021; Costa et al. 2021a). Recent studies have shown that morphological data alone may fail to support important monophyletic units (Katz et al. 2018) correctly place species in their respective clades (Costa et al. 2021b). The present study is the first to record a case of striking ontogenetic colouration change in mountain catfishes of the genus *Trichomycterus*, revealed only after checking DNA sequences of individuals exhibiting different colouration phenotypes, again highlighting the importance of combining morphological and molecular data in trichomycterine taxonomical studies.

Acknowledgments: This work and the new species names have been registered with ZooBank under urn:lsid:zoobank.org:pub:6CE80DA0-FB23-46CE-B6BA-2F10D7C7AF16. We are grateful to Claudia P. Bove and Bruno B. Costa for help on the 2001 and 2003 collecting trips, and to Beatriz Mesquita on the 2020 trip, and to Caio R. M. Feltrin for providing comparative material. The manuscript benefitted from the criticisms provided by two anonymous reviewers. This work was supported by Conselho Nacional de Desenvolvimento Científico e Tecnológico (CNPq; grant 304755/2020-6 to WJEMC), Fundação Carlos Chagas Filho de Amparo à Pesquisa do Estado do Rio de Janeiro (FAPERJ; grant E-26/202.328/2018 to JLOM, E-26/202.005/2020 to AMK and E-26/201.213/2021 to WJEMC), and Coordenação de Aperfeiçoamento de Pessoal de Nível Superior (CAPES; Finance Code 001) through Programa de Pós-Graduação em: Biodiversidade

e Biologia Evolutiva /UFRJ; Genética/UFRJ; and Zoologia, Museu Nacional/UFRJ.

Authors' contributions: WJEMC: conceptualization, project administration, writing original draft; WJEMC and JLOM: phylogenetic analyses; WJEMC, JLOM, PFA, and AMK: field studies; WJEMC, JLOM, SL, and AMK: investigation, laboratory analyses; WJEMC, JLOM, and AMK: funding acquisition, visualization.

Competing interests: W.J.E.M.C., J.L.O.M, S.L., P.F.A., and A.M.K. declare that they have no conflict of interest.

Availability of data and materials: All molecular data and specimens analysed are available in the GenBank database and in the fish collection of Institute of Biology, Federal University of Rio de Janeiro, Rio de Janeiro (UFRJ).

Consent for publication: Not applicable.

Ethics approval consent to participate: This study follows all legal requirements; collection permits were provided by ICMBio (Instituto Chico Mendes de Conservação da Biodiversidade; permit number: 38553-7); field methods were approved by CEUA-CCS-UFRJ (Ethics Committee for Animal Use of Federal University of Rio de Janeiro; permit number: 065/18).

REFERENCES

- Angulo A, DoNascimento C, Lasso-Alcalá OM, Farah-Pérez A, Langeani F, Mcmahon CD. 2018. Redescription of *Trichomycterus striatus* (Meek & Hildebrand, 1913) (Siluriformes: Trichomycteridae), with notes on its geographic distribution. *Zootaxa* **4420**:530–550. doi:10.11646/zootaxa.4420.4.5.
- Antonelli A, Kissling WD, Flantua SGA, Bermúdez MA, Mulch A, Muellner-Riehl AN, Kreft H, Linder HP, Badgley C, Fjeldsã J, Fritz SA, Rahbek C, Herman F, Hooghiemstra H, Hoorn C. 2018. Geological and climatic influences on mountain Biodiversity. *Nat Geosci* **11**:718–725. doi:10.1038/s41561-018-0236-z.
- Ardila Rodríguez CA. 2011. *Trichomycterus ballesterosi* (Siluriformes: Trichomycteridae), especie nueva de la cuenca alta del Río Sinú, Colombia. *Dahlia* **11**:3–12.
- Barbosa MA, Costa WJEM. 2008. Description of a new species of catfish from the upper rio Paraíba do Sul basin, south-eastern Brazil (Teleostei: Siluriformes: Trichomycteridae) and re-description of *Trichomycterus itatayae*. *Aqua Internat J Ichthyol* **14**:175–186.
- Barbosa MA, Costa WJEM. 2010. Description of a new species of the catfish genus *Trichomycterus* (Teleostei: Siluriformes: Trichomycteridae) from the rio Paraíba do Sul basin, southeastern Brazil. *Vertebr Zool* **60**:193–197.
- Bockmann FA, Sazima I. 2004. *Trichomycterus maracaya*, a new catfish from the upper rio Paraná, southeastern Brazil (Siluriformes: Trichomycteridae), with notes on the *T. brasiliensis* species-complex. *Neotrop Ichthyol* **2**:61–74. doi:10.1590/S1679-62252004000200003.
- Chernomor O, von Haeseler A, Minh BQ. 2016. Terrace aware data structure for phylogenomic inference from supermatrices. *Syst Biol* **65**:997–1008. doi:10.1093/sysbio/syw037.
- Costa WJEM. 1992. Description de huit nouvelles espèces du genre *Trichomycterus* (Siluriformes: Trichomycteridae), du Brésil oriental. *Rev Fr Aquariol Herpetol* **18**:101–110.
- Costa WJEM. 2021. Comparative osteology, phylogeny and classification of the eastern South American catfish genus *Trichomycterus* (Siluriformes: Trichomycteridae). *Taxonomy* **1**:160–191. doi:10.3390/taxonomy1020013.
- Costa WJEM, Katz AM. 2021. Integrative taxonomy supports high species diversity of south-eastern Brazilian mountain catfishes of the *T. reinhardti* group (Siluriformes: Trichomycteridae). *Syst Biodiv* **19**:601–621. doi:10.1080/14772000.2021.1900947.
- Costa WJEM, Katz AM, Mattos JLO, Amorim PF, Mesquita BO, Vilardo PJ, Barbosa MA. 2020a. Historical review and redescription of three poorly known species of the catfish genus *Trichomycterus* from south-eastern Brazil (Siluriformes: Trichomycteridae). *J Nat Hist* **53**:2905–2928. doi:10.1080/00222933.2020.1752406.
- Costa WJEM, Mattos JLO, Amorim PF, Vilardo PJ, Katz AM. 2020b. Relationships of a new species support multiple origin of melanism in *Trichomycterus* from the Atlantic Forest of south-eastern Brazil (Siluriformes: Trichomycteridae). *Zool Anz* **288**:74–83. doi:10.1016/j.jcz.2020.07.004.
- Costa WJEM, Mattos JLO, Katz AM. 2021a. Two new catfish species from central Brazil comprising a new clade supported by molecular phylogeny and comparative osteology (Siluriformes: Trichomycteridae). *Zool Anz* **293**:124–137. doi:10.1016/j.jcz.2021.05.008.
- Costa WJEM, Mattos JLO, Katz AM. 2021b. Phylogenetic position of *Trichomycterus payaya* and examination of osteological characters diagnosing the Neotropical catfish genus *Ituglanis* (Siluriformes: Trichomycteridae). *Zool Stud* **60**:43. doi:10.6620/ZS.2021.60-43.
- Felsenstein J. 1985. Confidence limits on phylogenies: an approach using the bootstrap. *Evolution* **39**:783–791. doi:10.1111/j.1558-5646.1985.tb00420.x.
- Ferrer J, Malabarba LR. 2013. Taxonomic review of the genus *Trichomycterus* Valenciennes (Siluriformes: Trichomycteridae) from the laguna dos Patos system, Southern Brazil. *Neotrop Ichthyol* **11**:217–246. doi:10.1590/S1679-62252013000200001.
- Fujisawa T, Barraclough TG. 2013. Delimiting species using single-locus data and the generalized mixed Yule coalescent approach: a revised method and evaluation on simulated data sets. *Syst Biol* **62**:702–724. doi:10.1093/sysbio/syt033.
- Hoang DT, Chernomor O, von Haeseler A, Minh BQ, Vinh LS. 2018. UFBoot2: Improving the ultrafast bootstrap approximation. *Mol Biol Evol* **35**:518–522. doi:10.1093/molbev/msx281.
- Hoorn C, Mosbrugger V, Mulch A, Antonelli A. 2013. Biodiversity from mountain building. *Nat Geosci* **6**:154. doi:10.1038/ngeo1742.
- Katz AM, Barbosa MA, Mattos JLO, Costa WJEM. 2018. Multigene analysis of the catfish genus *Trichomycterus* and description of a new South American trichomycterine genus (Siluriformes, Trichomycteridae). *Zoosyst Evol* **94**:557–566. doi:10.3897/zse.94.29872.
- Kumar S, Stecher G, Li M, Knyaz C, Tamura K. 2018. MEGAX: Molecular Evolutionary Genetics Analysis across computing platforms. *Mol Biol Evol* **35**:1547–1549. doi:10.1093/molbev/msy096.
- Lanfear R, Frandsen PB, Wright AM, Senfeld T, Calcott B. 2016. PartitionFinder 2: new methods for selecting partitioned models

- of evolution for molecular and morphological phylogenetic analyses. *Mol Biol Evol* **34**:772–773. doi:10.1093/molbev/msw260.
- Miranda Ribeiro A. 1905. Vertebrados do Itatiaya (peixes, serpentes, sáurios, aves e mamíferos): resultados de excursões do Sr. Carlos Moreira, assistente da Secção de Zoologia do Museu Nacional. *Arch Mus Nac* **13**:165–190 + 3 pls.
- Nguyen LT, Schmidt HA, von Haeseler A, Minh BQ. 2015. IQ-TREE: A fast and effective stochastic algorithm for estimating maximum likelihood phylogenies. *Mol Biol Evol* **32**:268–274. doi:10.1093/molbev/msu300.
- Rambaut A, Drummond AJ, Xie D, Baele G, Suchard MA, Rambaut A, Drummond AJ, Xie D, Baele G, Suchard MA. 2018. Posterior summarisation in Bayesian phylogenetics using Tracer 1.7. *Syst Biol* **67**:901–904. doi:10.1093/sysbio/syy032.
- Ribeiro AC. 2006. Tectonic history and the biogeography of the freshwater fishes from the coastal drainages of eastern Brazil: an example of faunal evolution associated with a divergent continental margin. *Neotrop Ichthyol* **4**:225–246. doi:10.1590/S1679-62252006000200009.
- Ritchie AM, Lo N, Ho SYW. 2017. The impact of the tree prior on molecular dating of data sets containing a mixture of inter- and intraspecies sampling. *Syst Biol* **66**:413–425. doi:10.1093/sysbio/syw095.
- Sazima I. 2004. Natural history of *Trichogenes longipinnis*, a threatened trichomycterid catfish endemic to Atlantic forest streams in southeast Brazil. *Ichthyol Explor Freshw* **15**:49–60.
- Schwarz G. 1978. Estimating the dimension of a model. *Ann Statist* **6**:461–464. doi:10.1214/aos/1176344136.
- Suchard MA, Lemey P, Baele G, Ayres DL, Drummond AJ, Rambaut A. 2018. Bayesian phylogenetic and phylodynamic data integration using BEAST 1.10. *Virus Evol* **4**:vey016. doi:10.1093/ve/vey016.
- Taylor WR, Van Dyke GC. 1985. Revised procedures for staining and clearing small fishes and other vertebrates for bone and cartilage study. *Cybium* **9**:107–119.
- Vilardo PJ, Katz AM, Costa WJEM. 2020. Relationships and description of a new species of *Trichomycterus* (Siluriformes: Trichomycteridae) from the Rio Paraíba do Sul basin, southeastern Brazil. *Zool Stud* **59**:53. doi:10.6620/ZS.2020.59-53.
- Villa-Verde L, Lazzarotto H, Lima SQM. 2012. A new glanapterygine catfish of the genus *Listrura* (Siluriformes: Trichomycteridae) from southeastern Brazil, corroborated by morphological and molecular data. *Neotrop Ichthyol* **10**:527–538. doi:10.1590/S1679-62252012000300005.
- Zanata AM, Primitivo C. 2013. Natural history of *Copionodon pecten*, an endemic trichomycterid catfish from Chapada Diamantina in northeastern Brazil. *J Nat Hist* **48**:203–228. doi:10.1080/00222933.2013.809168.
- Zhang J, Kapli P, Pavlidis P, Stamatakis A. 2013. A general species delimitation method with applications to phylogenetic placements. *Bioinform* **29**:2869–2876. doi:10.1093/bioinformatics/btt499.